

Electric-field-induced Raman scattering: Resonance, temperature, and screening effects

F. Schäffler* and G. Abstreiter

Physik-Department E16, Technische Universität München, D-8046 Garching bei München, Federal Republic of Germany

(Received 4 October 1985; revised manuscript received 28 May 1986)

A comprehensive, experimental characterization of electric-field-induced Raman scattering (EFIRS), a method to probe electric fields within a semiconductor depletion region, is given. Resonance effects, screening of the depletion region by photoexcited carriers, and the influence of temperature on the Raman signal of the symmetry-forbidden, electric-field-dependent LO phonon are discussed for the case of cleaved *n*-type GaAs surfaces. By comparing results from biased Schottky devices with those from adsorbate-covered surfaces, which were cleaved in ultrahigh vacuum, it is shown that the theoretically expected linear relation between the LO-phonon Raman signal and the Schottky-barrier height holds for the whole range of adsorbate-related potential barriers. In extreme resonance, higher-order effects can affect this relation drastically. However, choosing appropriate power densities of the exciting laser source leads to a partial screening of the space-charge layer by photoexcited carriers, which strongly attenuates these nonlinear effects. Hence a relatively simple calibration of the Raman signals in terms of absolute barrier heights becomes possible by using well-established Schottky-barrier heights as a calibration standard.

I. INTRODUCTION

The presence of an electric field within the probed volume of a Raman experiment leads in polar crystals to an additional higher-order mechanism for inelastic scattering by LO phonons.¹⁻⁸ This kind of electric-field-induced Raman scattering (EFIRS) permits, for example, to probe changes of the electric fields in space-charge layers at semiconductor surfaces and interfaces. The use of that technique is especially interesting for *in situ* studies of Schottky-barrier formation and to trace the development of the potential barrier at the interface of semiconductor heterojunctions. Compared to traditional photoemission spectroscopy (PES) and contact-potential difference (CPD) measurements, which are widely used in this field, EFIRS has the advantage of a much larger information depth, due to both the larger light-penetration depth with respect to the electron-escape depth of PES and the fact that the electric field in the semiconductor is probed rather than core-level shifts, which can be affected by chemical shifts and interdiffusion processes.⁹ The latter effects restrict PES measurements to coverages of about 10 Å thickness, while CPD techniques are limited to about one monolayer (ML).¹⁰ EFIRS, on the other hand, can be used up to several 100-Å thick overlayers,^{11,12} thus closing the information gap between conventional *in situ* methods and electrical *I-V* and *C-V* measurements, which require thick overlayers. Though several adsorbates pin the Fermi level at low coverages,¹³ this intermediate range can be important, e.g., in the case of the Al/GaAs interface, where low-coverage PES experiments and electrical measurements result in different barrier heights.¹³ Another example is the epitaxially grown Ge/GaAs interface, where PES experiments led to the erroneous interpretation of Fermi-level pinning at the interface,¹⁴ because the low-coverage experiments failed to distinguish between pinning at the Ge surface and at the interface. This result

was in contradiction to the experimental observation of a two-dimensional electron gas at the Ge side of the junction,¹⁵ and indeed a subsequent EFIRS experiment showed that epitaxially grown Ge forms an unpinned interface on GaAs.¹¹

So far, the application of EFIRS was mostly restricted to trace relative changes in band bending by following the change of the LO-phonon Raman signal as a function of adsorbate coverage of a cleaved III-V compound semiconductor surface. Giving quantitative values for the barrier height was somewhat problematic, as there were only a few systematic studies available which investigated the influence of experimental parameters on the intensity of the field-induced LO-phonon signal.¹⁶ The purpose of this contribution is to present a comprehensive study of the relevant parameters that might affect the predicted linear relation between the field-induced LO-phonon signal I_{LO} and the square of the electric field \mathcal{E}^2 , and thus the interpretation of EFIRS results. As *in situ* EFIRS experiments are usually performed under conditions of resonant excitation to keep signal-averaging times short, and as the experiment itself creates electron-hole pairs in the depletion layer, we concentrate mainly on resonance and screening effects, which are studied at different temperatures. The results are presented and discussed in Sec. III, preceded by a brief review of the basic mechanisms responsible for EFIRS in Sec. II.

II. BASIC ASPECTS OF EFIRS

First-order Raman scattering by LO phonons is symmetry forbidden in back scattering configuration from the (110) cleavage plane of zinc-blende-type semiconductors.¹⁷ Excitation close to resonance, however, enhances higher-order mechanisms, which do not necessarily obey the same selection rules. Two independently acting mechanisms of that kind have been discussed for "forbidden"

LO-phonon scattering in polar III-V compound semiconductors.¹⁸ Both are based on the Fröhlich interaction, i.e., the coupling between an excited electron-hole pair and the longitudinal electric field associated with a LO phonon. One mechanism is the well-known q -dependent Fröhlich term (q is the scattering wave vector) that leads to a scattering crosssection $\partial\sigma/\partial\omega \sim q^2$, which vanishes for $q=0$.¹⁸ Due to the small scattering wave vector involved in optical experiments and because of the mainly covalent bonding character, the q -dependent Fröhlich contribution to the one-phonon Raman spectrum is small in III-V compound semiconductors, but q -nonconserving mechanisms like impurity scattering can enhance that process close to resonance. If a static electric field \mathcal{E} is present within the scattering volume, the photoexcited electron-hole pairs become polarized, leading to an \mathcal{E} -dependent, q -independent contribution to the Fröhlich mechanism.

EFIRS has been treated theoretically by Gay *et al.*^{6,7} and by Zeyher *et al.*⁸ They both find in the case of low electric fields \mathcal{E} a Raman-scattering cross section $\partial\sigma/\partial\omega \sim \mathcal{E}^2$, where \mathcal{E} is the component of \mathcal{E} parallel to q . For higher fields a flattening of the \mathcal{E}^2 behavior is expected but has not been treated quantitatively, because of the limited range of field strength, where the perturbation ansatz of Gay *et al.* is valid.⁶ An experimental investigation of this question will be given in Sec. III.

Pinczuk and Burstein were the first to show that EFIRS can be used to probe the electric field within the surface depletion layer of a polar semiconductor.³ Apart from a small region at the end of the depletion layer, which is slightly affected by free carriers,¹⁹ the field and potential variation can be very well approximated by the simple Schottky model. In this analytic formulation one gets for $z \leq z_0$ (without image potential and finite-temperature correction)²⁰

$$z_0 = \left[2 \frac{\epsilon_s}{eN_D} V_b \right]^{1/2}, \quad (1)$$

$$|\mathcal{E}(z)| = e \frac{N_D}{\epsilon_s} (z_0 - z), \quad (2)$$

$$V(z) = e \frac{N_D}{2\epsilon_s} (z_0 - z)^2, \quad (3)$$

where z_0 is the length of the abruptly terminated depletion region, V_b is the potential at the surface ($z=0$), N_D is the bulk doping concentration, ϵ_s is the static dielectric constant of the semiconductor, and e is the free-electron charge.

Equations (1), (2), (3) have two important implications. (i) The electric field decreases linearly with z . Therefore, if one is interested in probing this field with EFIRS, the penetration depth of the incident laser light should be small compared to z_0 . (ii) The square of the maximum electric field at $z=0$ is proportional to the potential barrier V_b . Hence, in the low-field limit, where the Raman signal is expected to be proportional to \mathcal{E}^2 , and with (i) fulfilled, the LO-phonon Raman signal directly reflects the Schottky-barrier height.

In moderately doped ($\leq 10^{18} \text{ cm}^{-3}$) III-V compound semiconductors the light penetration depth δ is smaller

than z_0 , if the E_1 gap (the two-dimensional critical point of the band structure) is chosen for resonant excitation. In the case of GaAs the relevant parameter is $\delta \equiv 1/2\alpha \simeq 85 \text{ \AA}$, where α is the light-absorption constant at $\hbar\omega = 3.0 \text{ eV} \simeq E_1$ (Ref. 21) and the factor of 2 arises from the backscattering geometry. This leads to an intensity of the LO-phonon signal of

$$I_{\text{LO}} \sim \int_0^\infty \mathcal{E}^2(z) e^{-z/\delta} dz. \quad (4)$$

An evaluation of (4) shows that $I_{\text{LO}} \sim V_b$ within 10% for $V_b > 50 \text{ mV}$ and a doping concentration $N_D \leq 7 \times 10^{17} \text{ cm}^{-3}$. On the other hand, (4) is only a crude description of the I_{LO} versus V_b relation, as neither a possible saturation of the \mathcal{E}^2 behavior of I_{LO} nor screening effects due to the photoexcited electron-hole pairs are included. Both effects will be discussed in more detail in Sec. III.

III. EXPERIMENTAL CHARACTERIZATION OF EFIRS

To derive quantitative values for the Schottky-barrier height as a function of surface coverage with adsorbates from an EFIRS experiment, the influence of several parameters on I_{LO} has to be known precisely: (i) linearity of I_{LO} versus V_b , (ii) resonance behavior, (iii) dependence on the power density of the incident laser light, (iv) temperature dependence, and (v) influence of the doping concentration of the semiconductor.

The first four parameters will be treated in the following for the case of n -type GaAs (110) surfaces. The dependence of the EFIRS signal on the doping concentration has been discussed in an earlier work,²² which showed that I_{LO} increases with the doping concentration because of the $\sqrt{N_D}$ dependence of the surface electric field. This results directly from Eqs.(1) and (2), assuming a constant barrier height V_b . The N_D dependence restricts the doping range where EFIRS can be used for a quantitative evaluation of Schottky barriers to about $1 \times 10^{17} \text{ cm}^{-3}$ up to some 10^{18} cm^{-3} . For lower doping concentrations the electric field in the depletion layer and hence the field-induced LO-phonon signal becomes so small that severe signal-to-noise problems result. For higher doping, the depletion length z_0 becomes of the order of δ or even smaller. For these reasons, we have mainly used $7 \times 10^{17} \text{ cm}^{-3}$ Te-doped GaAs samples from the same crystal, to allow a direct comparison of the EFIRS signals.

Most of the experiments were performed in a stainless-steel ultrahigh vacuum (UHV) chamber with a base pressure of $\leq 5 \times 10^{11} \text{ Torr}$. A double-notch/double-wedge cleaving facility and an oxygen leak valve allowed for *in situ* studies of clean and oxygen exposed (110) surfaces. In addition, metals could be evaporated at very low and defined rates from effusion cells with pyrolytic BN crucibles. The samples could be cooled to $\simeq 85 \text{ K}$. Experiments with Schottky devices were performed in a temperature-controlled liquid nitrogen cryostat. For all Raman measurements a standard equipment, consisting of Kr⁺-ion laser and Stilben 3 dye laser, a double-grating spectrometer, and a photomultiplier with associated

pulse-counting electronics has been used. Experiments were performed in backscattering configuration with the polarization vectors of incoming and scattered light chosen both parallel to the $(1\bar{1}0)$ direction of the crystal. In this geometry TO-phonon scattering, which is virtually not affected by electrical fields, is symmetry allowed¹⁷ and the corresponding signal I_{TO} was used to normalize the “forbidden” LO-phonon signal I_{LO} .

A. Resonance behavior and relation between I_{LO} and V_b

To test the resonance behavior of EFIRS as a function of an electric field within the scattering volume we performed Raman experiments with Schottky devices, which allow the surface electric field to be tuned continuously. The diodes have been fabricated by evaporating semitransparent Au or Ni-Cr contacts onto GaAs(110) surfaces, which were prepared by cleaving GaAs crystals at atmospheric pressure and introducing the samples immediately into a conventional evaporation system. Mechanical masks were used, leading to typical contact areas of 0.4 mm^2 . Ohmic Sn contacts have been alloyed to the semiconductor prior to cleaving to avoid any heat treatment of the devices. The samples were Te-doped with a doping concentration of $1.3 \times 10^{17} \text{ cm}^{-3}$, lower than those used for the UHV experiments described below, to achieve higher breakdown voltages of the diodes, and to assure that $z_0 \gg \delta$. As laser illumination of the samples during the Raman experiments unavoidably leads to a photocurrent across the Schottky contact, the voltage drop along the semitransparent metal gates with a typical sheet resistance of $1\text{--}5 \text{ k}\Omega_{\square}$ was corrected by using two contacts on the gate area. The bias voltage was applied to one of these, while the other was used for high-impedance probing of the actual voltage drop across the junction at the laser-illuminated spot. The diodes were characterized by I - V and C - V measurements and selected for low reverse current and high breakdown voltage. Typical barrier heights were $V_b \simeq 0.8 \text{ eV}$.

Figure 1 shows two sets of Raman data for device temperatures of 300 and 85 K. The curves represent the normalized EFIRS signal I_{LO}/I_{TO} for various laser energies around the respective temperature-dependent E_1 -gap energy as a function of the voltage drop at the laser focus. A strong resonance behavior is observed for both temperatures: Close to the resonance maximum (respective top-most curves in Fig. 1; compare also Fig. 3), the forbidden LO-phonon signal reaches maximum values that are comparable to the allowed TO-phonon signal at 300 K, and becomes up to 4.5 times larger at 85 K. Besides the strong enhancement, it is obvious that close to resonance the relation between I_{LO}/I_{TO} and the effective interface potential $V = V_{\text{bias}} - V_b$ is strongly nonlinear. While the room-temperature curves show saturation, which moves to lower electric fields as the excitation approaches the E_1 gap, the in-resonance curves at 85 K show even a decrease at higher fields. This finding seems to be in contradiction to the expected linear increase of I_{LO}/I_{TO} with increasing reverse-bias voltage that has been discussed in Sec. II. On the other hand, the respective lower curves in Fig. 1, which were recorded slightly ($\leq 150 \text{ meV}$) out of reso-

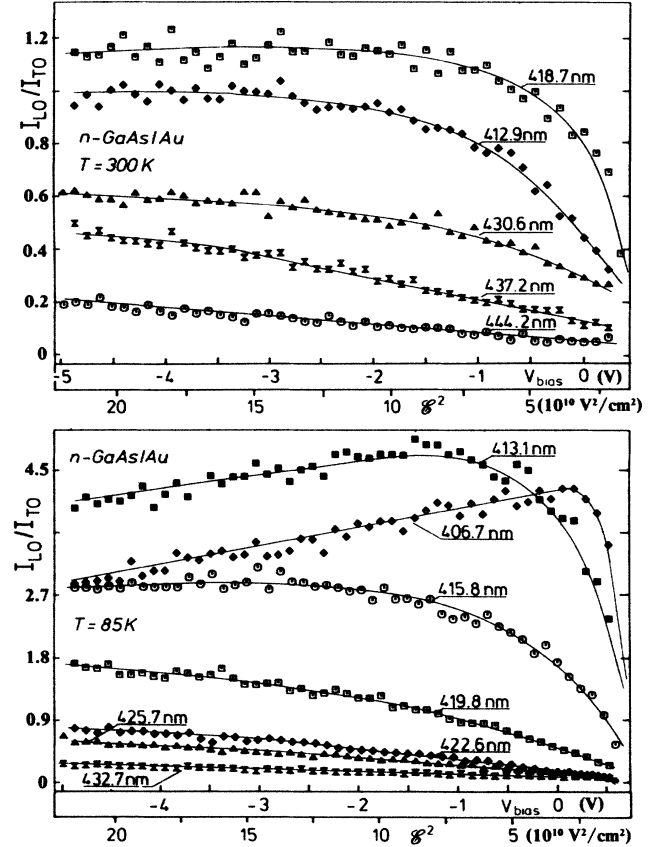


FIG. 1. Dependence of the normalized LO-phonon Raman signal I_{LO}/I_{TO} on the bias voltage applied to Schottky devices with semitransparent gates for various laser energies around the E_1 gap of GaAs. The upper graph shows data at room temperature, the lower at 85 K.

nance, show that the observed nonlinear behavior is a resonance-related effect rather than an intrinsic deviation from the predicted \mathcal{E}^2 behavior: Those curves, which are in agreement with an earlier off-resonance experiment,¹⁶ give a strictly linear dependence of the EFIRS signal on V within the range of field strength available with our Schottky devices.

What are the resonance effects that cause a saturation of I_{LO} at relatively low fields, and, in extreme low-temperature resonance, even a decrease of I_{LO} as a function of \mathcal{E}^2 ? One possible effect is the Franz-Keldysh mechanism,^{23,24} which leads to a modification of the valence- and conduction-band electron wave functions in an electric field. While this effect allows q -independent Fröhlich interaction—and therefore EFIRS—due to the polarization of the photoexcited electron-hole pairs,⁴ it also lowers the optical band gap, as the exponential damped tails of the wave functions leak into the band gap when the bands are tilted in an electric field. This band gap lowering shifts the resonance position to lower energies with increasing field. Thus, in an experiment as described above, where the exciting laser energy remains

constant while the electric field is varied, the detuning of the resonance condition is expected to result in an artificial modification of the observed relation between I_{LO} and \mathcal{E}^2 . This argument is supported by the fact that the absolute intensity of the TO-phonon signal, which is virtually field independent slightly out of resonance, is attenuated at higher fields, when excited under resonant conditions. This effect is small at room temperature (less than 10% over the field range in Fig. 1), but can become significant in extreme low-temperature resonance (Fig. 2).

To determine the importance of the Franz-Keldysh bandgap lowering for the observed deviations of I_{LO} from the \mathcal{E}^2 behavior, resonance curves were measured for various values of bias voltage applied to the Schottky diodes. Two sets of such curves are shown in Fig. 3 for temperatures of 300 and 85 K, respectively. The negative bias voltage was increased by a constant amount from one set of data points to the next. Though we did not fit the data to a certain line shape, as there are two critical points within the frequency range examined²⁵ (E_1 and $E_1 + \Delta_1$), care has been taken when drawing the lines through the data points to give a guide for the relative changes in the resonance profile.

Figure 3 shows for both temperatures the expected shift to lower energies with increasing fields. This is clearly visible for the 85-K data, where the data points on the high-energy side show decreasing phonon intensity with increasing field, while those on the low-energy side show increasing intensity (compare Fig. 1). A similar but less pronounced behavior is observed in the room-temperature data, especially in the two sets of data points on either side of the resonance maximum, which is again consistent with a resonance shift to lower energies. Nevertheless, the Franz-Keldysh shift appears to be too small to explain the resonance behavior of Fig. 1 completely: Both panels in Fig. 3 show a sublinear increase of I_{LO}/I_{TO} next to the resonance maximum on its low-energy side. As V_{bias} (and therefore \mathcal{E}^2) increases linearly from one curve to the other, the field-induced contribution alone would lead to a linear increase of I_{LO}/I_{TO} , and the resonance shift should

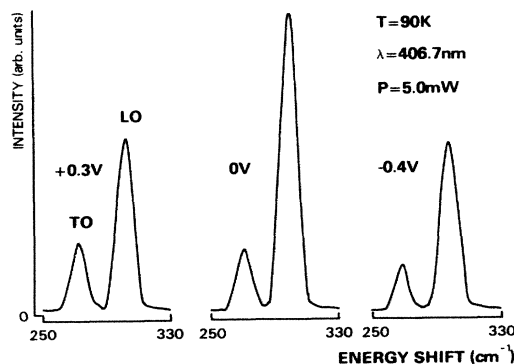


FIG. 2. Raman spectra of the optical phonons for various bias voltages applied to a GaAs Schottky device. Laser excitation is resonant for the device temperature of 85 K, leading to a noticeable field dependence of the TO-phonon signal, which is not observed slightly out of resonance.

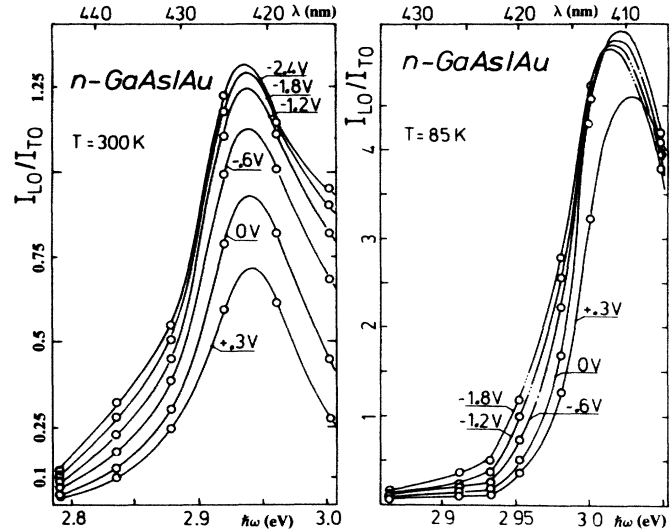


FIG. 3. Resonance behavior of I_{LO}/I_{TO} at two temperatures for different values of V_{bias} , the voltage applied to the Schottky devices. Note the different scales on both axis, which are due to the temperature shift of the E_1 gap and the large resonance enhancement at low temperatures.

add intensity on the low-energy side. This is clearly not the case; instead, it appears that the resonance profile flattens with increasing fields, indicating that additional higher-order mechanisms interfere in a destructive manner with the field-dependent Fröhlich mechanism.

So far, little is known about such additional effects. However, it seems to be likely that there is a connection between the unusually large resonance enhancement—especially at low temperatures—and the nonlinearities in the EFIRS signal: This enhancement is larger than expected from theoretical treatments,⁸ and it has been speculated that E_1 -gap excitons are responsible for that discrepancy.^{3,8} As exciton lifetimes are strongly affected even by small electric fields,²⁶ a change in the resonance profile with increasing field appears plausible. Nevertheless, a more detailed understanding of the relevance of E_1 -gap excitons for resonant Raman scattering in GaAs is necessary.

B. Screening effects at adsorbate-covered surfaces

The resonance experiments with Schottky devices demonstrate that the electric-field-induced LO-phonon signal is proportional to the square of the field within the scattering volume, at least up to a field strength of $\geq 4 \times 10^5$ V/cm. This holds for laser excitation slightly out of resonance, while in extreme resonance higher-order mechanisms lead to deviations from the \mathcal{E}^2 relation. However, these results cannot be used to calibrate the phonon-intensity ratio I_{LO}/I_{TO} in terms of band bending at an adsorbate-covered semiconductor surface, because the laser illumination makes the two cases very different: The illuminated Schottky device behaves like a reverse-biased photodiode, while the adsorbate-covered, depleted

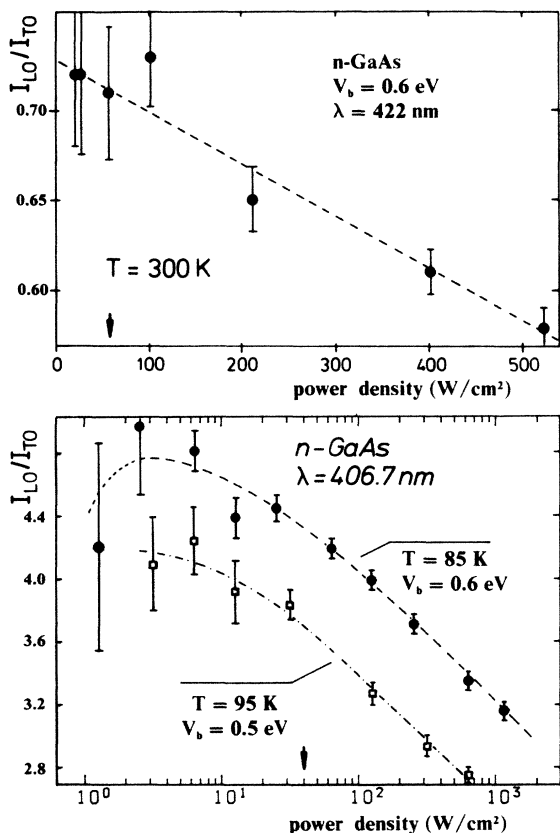


FIG. 4. Dependence of the EFIRS signal from depleted GaAs surfaces on the power density of the exciting laser radiation at different temperatures. The laser energies were chosen to match the respective, temperature-dependent resonance condition. The arrows indicate power densities that were used in most experiments. Note that the abscissa of the lower graph is scaled logarithmically.

semiconductor surface acts like a free-running solar cell. In the first case the applied voltage source keeps the interface potential constant, resulting in a photocurrent across the junction that depends on the power density of the laser light. This current causes some deviations of the parabolic potential variation of the Schottky model, but these effects are negligible for EFIRS experiments, as they mainly affect the transition region between depletion layer and semiconductor bulk,²⁷ i.e., a region that is outside the probing depth δ . We have tested the influence of the photocurrent on I_{LO}/I_{TO} by varying the light intensity and find only a slight shift of the curves in Fig. 1 which can be explained by the voltage drop across the relatively high-ohmic semiconductor bulk of our samples. Therefore, Schottky devices behave in EFIRS experiments virtually like nonilluminated Schottky barriers. On the other hand, no photocurrent is possible in adsorbate-covered semiconductors, but a photovoltage in opposite direction to the built-in Schottky barrier is established due to the separation of photoexcited electron-hole pairs in the electric field of the depletion region, i.e., the potential barrier becomes more and more screened with increasing laser-power density. This is clearly demonstrated by the experiments shown in Fig. 4: For oxygen exposed GaAs (110)

surfaces the dependence of I_{LO}/I_{TO} is plotted as a function of laser-power density. The measurements were performed at different temperatures, and the laser energy has been chosen to be close to the respective (temperature-dependent) resonance position (compare Fig. 3). The band bending was defined by oxygen exposure of the surfaces, and has been estimated to be ≈ 0.6 eV and 0.5 eV, respectively. At 300 K, I_{LO}/I_{TO} drops linearly with power density, while at low temperatures the dependence is exponential over a wide power-density range. Figure 4 reveals two important facts: (i) There is no tendency for a saturation of I_{LO}/I_{TO} with increasing power density, not even at 500 and 1000 W/cm², respectively, corresponding to 40 and 80 mW of absolute laser power in a point focus of ≈ 100 μ m. Therefore the Schottky barrier is far from being completely screened by photocarriers within the studied range. This result is also of some importance for the interpretation of surface photovoltage (SPV) measurements, where sometimes a complete screening of the illuminated Schottky barrier has been assumed in order to derive absolute barrier heights.²⁸ (ii) I_{LO}/I_{TO} shows saturation at very low power densities, but it is much harder to achieve this situation at low temperatures: The lowest absolute laser power used was 0.1 mW, corresponding to 1.2 W/cm², which leads to considerable signal-to-noise problems, as is indicated by the large error bar.

The measurements used for Fig. 4 were recorded very close to resonance, where the experiments with Schottky devices have shown pronounced deviations of I_{LO}/I_{TO} versus V from linearity. As the space-charge region is partly screened by photocarriers in the case of adsorbate-covered surfaces, it is interesting to compare the two cases directly. For this purpose, we have performed EFIRS experiments, where the surface electric field has been tuned by adsorbate-induced formation of Schottky barriers. As the atomically clean, "well" cleaved GaAs(110) surface is known to show flatband behavior ($V_b = 0$),²⁹ the surface electric field can be increased continuously by exposing the surface to, e.g., oxygen, or by carefully controlled evaporation of metals. The final field at the surface is determined by the doping concentration and by the adsorbate-dependent saturation barrier height [Eqs. (2) and (3)].

Two examples are shown in Fig. 5, one for samples exposed to oxygen at room temperature, the other for surfaces that were successively covered with small amounts of silver at 85 K. *n*-type doped GaAs samples with a carrier concentration of 7×10^{17} cm⁻³ were used. With that doping concentration and with a saturation barrier height of 0.63 eV (Ref. 30) for the case of oxygen exposure and ≈ 1 eV (Refs. 9 and 13) for silver, the Schottky model [Eqs. (1) and (2)] gives surface electric fields of 3.4×10^5 and 4.6×10^5 V/cm, respectively. Therefore, the same range of field strength is available as with the Schottky-device arrangement described above. The experiments were performed with the two violet laser lines of the Kr⁺-ion laser, with wavelengths of 413.1 and 406.7 nm. The first is quite close to the E_1 -gap energy at room temperature, while the latter is resonant at 100 K (compare Fig. 3). The x axes in Fig. 5 are scaled in units of Langmuir (1 L $\equiv 10^{-6}$ Torr) as a measure for oxygen exposure, and in angstroms of silver coverage, respectively. To

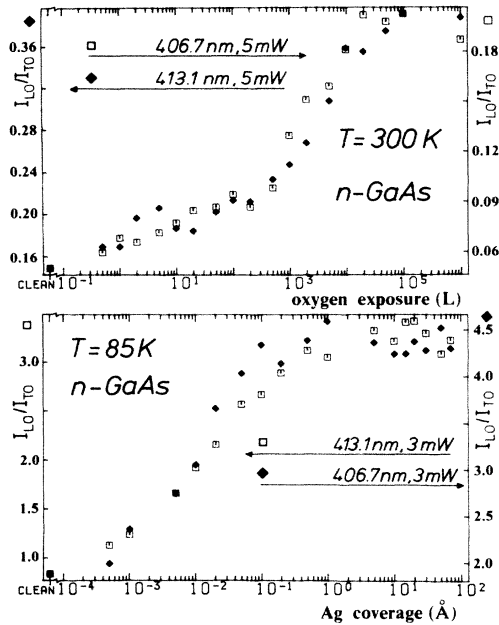


FIG. 5. EFIRS experiments at adsorbate covered *n*-type GaAs (110) surfaces. The upper part shows I_{LO}/I_{TO} for oxygen exposed samples at 300 K; for the lower graph Ag was evaporated onto samples held at 85 K. The different data sets in each frame correspond to laser excitation at 413.1 nm (3.00 eV) and 406.7 nm (3.05 eV).

permit a direct comparison of the related data sets despite the different proximity of the two laser lines to the respective resonance position, the data were normalized to the start value of I_{LO}/I_{TO} after cleaving and to a mean saturation value. The corresponding absolute scales for the phonon-intensity ratios are given on either side of the panels.

Figure 5 shows that the corresponding data agree within the statistical fluctuations for both temperatures studied, in contrast to the pronounced resonance behavior found at the Schottky diodes. Especially the most remarkable feature of the resonant low-temperature curves in Fig. 1, namely, the decrease of I_{LO}/I_{TO} at higher fields, is completely missing. On the other hand, the absolute values of I_{LO}/I_{TO} in Fig 5 are lower than the corresponding ones in Fig. 1, being roughly limited to the zero bias values in Fig. 1. This is more evident for the room-temperature data, where the saturation onset is less pronounced. For that bias voltage the barrier height is equal to the intrinsic value of ≈ 0.8 eV. This allows a crude estimation of the actual surface fields at the illuminated, adsorbate-covered surfaces: According to Eqs. (1) and (2), $\mathcal{E}(z=0)$ scales with $\sqrt{N_D}$. Using the two different doping concentrations for the devices and the UHV-cleaved samples, we find that the measured saturation fields at the adsorbate-covered surfaces are reduced by roughly a factor of 2 as an effect of laser illumination with power densities between 40 and 60 W/cm².

The direct comparison between the EFIRS measurements on Schottky devices and on adsorbate-covered sur-

faces shows that in the latter case screening by photoexcited carriers limits the surface electric fields to values below the onset of the nonlinear, higher-order effects, which lead to deviations from the \mathcal{E}^2 behavior very close to resonance. As the extent of screening depends on the steady-state concentration of photoexcited electron-hole pairs, the device results should be reproduced in the *limes* of vanishing laser intensity. Indeed, the dashed curve in the lower part of Fig. 4, where the power-density dependence of I_{LO}/I_{TO} has been studied at an oxygen exposed surface, indicates a lowering of the phonon-intensity ratio at very low light intensities. This is exactly what one expects from the low-temperature resonance behavior found for the diodes (compare curve measured with the 406.7-nm line in the lower part of Fig. 1): As screening becomes less important at low laser intensities, the actual surface field increases, reaching values where resonant higher-order effects cause a decrease of I_{LO}/I_{TO} .

To get a feeling for the screening properties of the photoexcited electron-hole pairs, we performed numerical calculations of the illuminated space-charge region. The simple quasiequilibrium model was used, which assumes the valence- and conduction-band carriers to be in a respective equilibrium situation, described by two quasi-Fermi-levels μ_n and μ_p .^{19,31} This model works quite well for indirect-gap semiconductors like Ge,³² but may give only a rough description in the case of GaAs, where radiative recombination is of importance. The calculations are therefore expected to reproduce trends rather than quantitative values.

In the case of homogeneous illumination of a depleted *n*-type GaAs sample, which is treated in the following, the quasi-Fermi-levels are defined by δp , the stationary density of excess minority carriers just at the end of the depletion layer.¹⁹ Acceptorlike surface states with a density parameter N_{ss} and a sharp energy level $E_{sa} = -0.7$ eV (with respect to the conduction-band minimum) are assumed. The population of surface states with electrons is determined by the electron quasi-Fermi-level. The localized nature of the surface states is simulated by giving the density distribution an exponentially decaying profile in the z direction of the form $e^{-z/d}$. The finite extension of these states becomes important in the case of an illuminated depletion layer, as the use of classical statistics leads to a narrow layer of excess minority carriers with the density maximum at $z=0$. This would create an unrealistic surface dipole if the surface states were treated two dimensionally.

Figure 6 shows results of our calculation: The variations of potential and electric field are plotted as a function of z and N_{ss} for the nonilluminated case ($\delta p=0$) and for a photo-induced excess hole concentration of $\delta p=10^{15}$ cm⁻³. The latter value has been chosen to give roughly a reduction of the saturation surface field by a factor of 2, as has been found in the experiments described above. By comparing the respective graphs for the illuminated and nonilluminated case, three main trends are recognizable: (i) Screening by photocarriers reduces, as expected, the values of \mathcal{E} and V_b , as well as the length of the depletion layer. (ii) Screening becomes more effective at higher V_b values, and therefore cannot be described by simply scal-

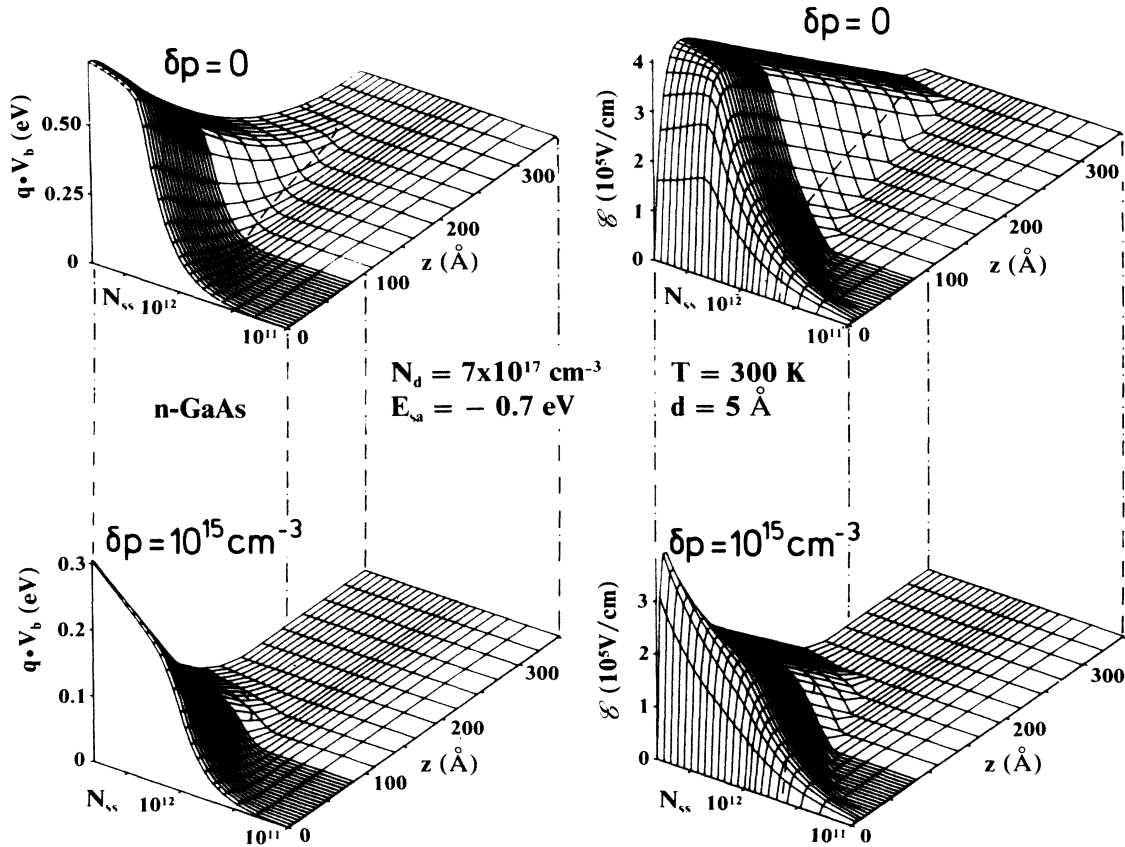


FIG. 6. Model calculation for the variation of potential and field within the depletion region of the illuminated Schottky barrier. $\delta\rho$ is a measure for the light intensity, with $\delta\rho=0$ corresponding to the nonilluminated case. The dashed lines show the position where the Fermi level crosses the conduction band, a consequence of *n*-type-GaAs being degenerated at the doping concentration chosen here. Note the nonlinear reduction of the illuminated space-charge region as a function of N_{ss} .

ing the Schottky model. (iii) At higher N_{ss} , the density of excess minority carriers close to $z=0$ increases rapidly, causing a sharp increase in \mathcal{E} and V_b within the first 50 Å of the depletion layer. This is, as mentioned above, mainly an artifact of our model, and depends to some extent on the value chosen for the decay length d of the surface states. It is expected that diffusion terms and quantum mechanical corrections will smear out the drastic field increase.

The calculated variation of $\mathcal{E}^2(z)$ can be used to evaluate the relative variation of I_{LO} as a function of N_{ss} according to Eq. (4): In the limes of vanishing illumination, which applies for experiments at biased Schottky devices, I_{LO} is fairly linear in V_b , as mentioned in Sec. II but shows a small increase in slope with increasing surface potential. This reflects the increasing extension of the space-charge layer with respect to the constant light penetration depth. That trend is reversed in the case of an illuminated surface, as screening becomes more efficient for higher values of V_b , leading to a sublinear I_{LO} versus V_b relation. At higher N_{ss} values the development of a surface dipole may affect these results, but a reasonable description of such effects is beyond the scope of our simple model.

C. Calibration of EFIRS

The simple calculations of screening effects in a space-charge layer show that some nonlinearities in I_{LO}/I_{TO} may be expected, but the model is too crude to derive quantitative values. A more sophisticated description is in principle possible,³¹ but every improvement is associated with new parameters, which are in most cases not well characterized by experiments. Therefore, we choose a more heuristic approach, exploiting an earlier experiment, that was performed to find a calibration standard for EFIRS experiments: In Ref. 12 we compared EFIRS experiments at oxygen exposed GaAs(110) surfaces with published CPD and PES results. Excellent agreement between the results of the three different techniques was found, by just assuming a linear relation between I_{LO}/I_{TO} and V_b without any corrections (Fig. 1 in Ref. 12). This means for our model calculation that there is obviously a large extent of cancellation between the effects of increasing depletion width and increasing screening efficiency. Moreover, the creation of a surface dipole appears to be overestimated by far in the simple calculation, and does obviously not affect the I_{LO}/I_{TO} versus V_b relation within the experimental uncertainties. Therefore we con-

clude that for the moderate power densities of 40–60 W/cm^2 (3–5 mW absolute in a 100- μm focus) used in our experiments the assumption of a linear relation between the EFIRS signal and the barrier height is an excellent approximation, which allows a relatively simple calibration in terms of absolute barrier heights.

Using an oxygen experiment as calibration standard is expected to give an absolute accuracy comparable to the uncertainties of PES measurements (≈ 100 mV) within the barrier-height range accessible by oxygen exposure.¹² Higher accuracy can be achieved by making use of several independent calibration points. For this purpose the recently published I - V and C - V measurements on devices prepared under UHV conditions on cleaved GaAs samples¹³ will be very helpful. Using these data seems to be especially advantageous for studying “high barrier” metals like Au, Ag, or Pd, which result in barriers of around 1 eV.¹³ In these cases the oxygen calibration would have to be extrapolated, resulting in unacceptable large error margins.¹² The use of device-derived barrier heights for additional calibration points rather than PES results also helps to overcome a source of systematic error of the latter technique in case of metal overlayers that show three-dimensional growth: The lateral potential inhomogeneities associated with such a growth mode can result in additional uncertainties of the order of 100 mV.^{9,33}

Despite the relative ease of calibration, it has to be pointed out that such a calibration is not universal: The discussion has shown that $I_{\text{LO}}/I_{\text{TO}}$ depends more or less pronounced on the exciting laser energy and its power density at the surface, the doping concentration of the sample and on temperature. Hence, it is necessary to repeat the procedure whenever one of these parameters has been changed. These factors limit also the relative resolution of EFIRS in terms of V_b , which basically depends on the signal-to-noise ratio of the two phonon signals and therefore on the four parameters that affect I_{LO} .

For temperature-dependent adsorption studies the calibration can easily be extended to any temperature by simply following $I_{\text{LO}}/I_{\text{TO}}$ for two definite barrier heights as a function of temperature. This is shown in Fig. 7 where the temperature dependence between 100 and 300 K is plotted for clean ($V_b \leq 100$ mV) and depleted surfaces with saturated barrier heights of ≈ 0.6 eV, reached after O_2 and NO exposure, respectively. Measurements in the upper part of the figure were performed with the 413.1-nm line, the lower ones at 406.7 nm. In both examples the laser power was kept constant at 5 mW absolute, corresponding to 60 W/cm^2 in a point focus of 100 μm diameter. A comparison of the two plots shows that the use of the 413.1-nm line is advantageous in the whole temperature range studied: The corresponding laser energy fulfills the E_1 -resonance condition at about 160 K, leading to relatively large Raman signals even at room temperature. At lower temperatures, the strong temperature dependence observed with the other laser line is diminished as the 413.1-nm line passes through resonance. Therefore, $I_{\text{LO}}/I_{\text{TO}}$ is only slightly temperature dependent between 100 and 160 K and beyond 260 K. This is important, as it is usually not convenient to attach a thermocouple to the UHV-cleaved surface. Therefore the

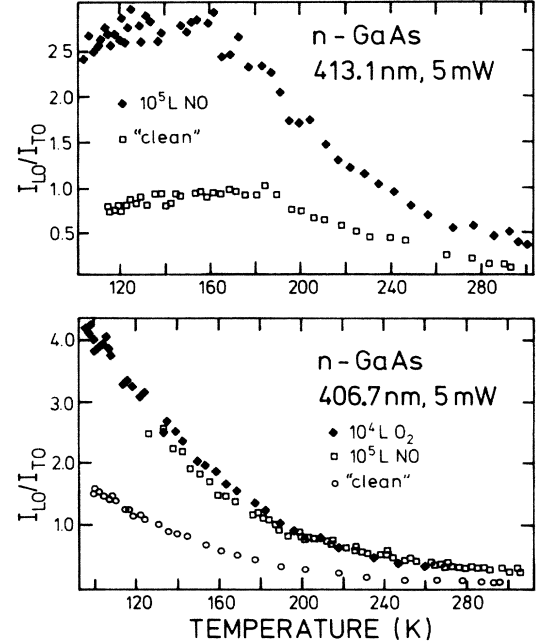


FIG. 7. Temperature dependence of $I_{\text{LO}}/I_{\text{TO}}$ for the two violet lines of a Kr^+ -ion laser. The two sets of data in each graph correspond to a potential barrier of 0.6 eV and to flatband. The LO-phonon intensity for the latter case results from the q -dependent term of the Fröhlich mechanism, that shows a similar resonance and temperature dependence as the field-induced mechanism.

temperature is in most cases measured somewhat remote from the surface, which may cause an error of the order of 10 K at lower temperatures. This is not acceptable when the 406.7-nm line is used because of the extreme temperature dependence of the Raman signal between 100 and 180 K, which is caused by the temperature dependence of forbidden LO-phonon scattering itself in addition to the increasing resonance enhancement when the temperature approaches 100 K, the approximate value where the 406.7-nm line matches the optical E_1 gap (compare Fig. 3).

IV. CONCLUDING REMARKS

The purpose of this contribution was to give a comprehensive experimental characterization of EFIRS and the parameters that influence the Raman signal of the field-induced LO-phonon. By comparing results from biased Schottky devices with those from adsorbate-covered surfaces, we could show that the theoretically predicted linear relation between the field-induced LO-phonon signal and the Schottky-barrier height holds for the entire range of surface fields accessible by adsorbate-related Fermi-level pinning at n -GaAs(110) surfaces. Close to resonance, however, additional mechanisms lead to significant deviations of the linear relation already at moderate electric fields. These mechanisms, which affect also scattering by TO-phonons, are not well understood as

yet. Additional effort is necessary, especially to achieve a better understanding of the unusual strong resonance enhancement, which has been speculated to be related to E_1 -gap excitons. For the application of EFIRS these nonlinearities can be strongly suppressed by choosing proper power densities of the exciting laser radiation, which leads to a partial screening of the potential barrier at the semiconductor surface, limiting the electric fields to values where nonlinear effects are not important. Additional nonlinearities, which are expected to be introduced by the screening properties itself, are smaller than the experimental uncertainties involved in the standard CPD and PES experiments used for comparison. Therefore, even under conditions of resonant excitation, which are

desirable to keep signal averaging times short, the assumption of a linear relation between Schottky barrier height and electric-field-induced LO-phonon signal is an excellent approximation, which allows a relatively simple calibration of the EFIRS signal in terms of absolute barrier heights. The calibration can easily be extended to different temperatures.

ACKNOWLEDGMENTS

This work has been supported by the Deutsche Forschungsgemeinschaft (Bonn, Germany) via Sonderforschungsbereich 128.

*Present address: IBM Thomas J. Watson Research Center, P.O. Box 218, Yorktown Heights, NY 10598.

¹P. A. Fleury, and J. M. Worlock, *Phys. Rev.* **174**, 613 (1968).

²J. F. Scott, P. A. Fleury, and J. M. Worlock, *Phys. Rev.* **177**, 1288 (1969).

³A. Pinczuk and E. Burstein, *Phys. Rev. Lett.* **21**, 1073 (1968).

⁴A. Pinczuk and E. Burstein, in *Proceedings of the 10th International Conference on the Physics of Semiconductors* (U.S. Atomic Energy Commission, Washington, D.C., 1971), p. 727.

⁵G. Abstreiter, M. Cardona, and A. Pinczuk, in *Light Scattering in Solids IV*, Vol. 54 of *Topics in Applied Physics*, edited by M. Cardona, and G. Güntherodt (Springer, Berlin, 1984).

⁶J. G. Gay, J. D. Dow, E. Burstein, and A. Pinczuk, in *Light Scattering in Solids*, edited by M. Balkanski (Flammarion Sciences, Paris, 1971).

⁷M. L. Shand, W. Richter, E. Burstein, and J. G. Gay, *J. Nonmetals* **1**, 53 (1972).

⁸W. Richter, R. Zeyher, and M. Cardona, *Phys. Rev. B* **18**, 4312 (1978).

⁹R. Ludeke, *Surf. Sci.* **168**, 290 (1986).

¹⁰J. M. Palau, E. Testemale, A. Ismail, and L. Lassabatère, *J. Vac. Sci. Technol.* **19**, 192 (1981).

¹¹H. Brugger, F. Schäffler, and G. Abstreiter, *Phys. Rev. Lett.* **52**, 141 (1984).

¹²F. Schäffler and G. Abstreiter, *J. Vac. Sci. Technol. B* **3**, 1184 (1985).

¹³N. Newman, M. van Schilfgaarde, T. Kendelewicz, M. D. Williams, and W. E. Spicer, *Phys. Rev. B* **33**, 1146 (1986), and references therein.

¹⁴W. Mönch, R. S. Bauer, J. Gant, and R. Murschall, *J. Vac. Sci. Technol.* **21**, 498 (1982).

¹⁵R. Merlin, A. Pinczuk, and C. E. E. Wood, *J. Vac. Sci. Technol.* **21**, 516 (1982).

¹⁶R. Trommer, G. Abstreiter, and M. Cardona, *Proceedings of the International Conference on Lattice Dynamics*, edited by M. Balkanski (Flammarion Sciences, Paris, 1977), p. 189.

¹⁷R. Loudon, *Adv. Phys.* **13**, 423 (1964).

¹⁸See, e.g., M. Cardona, in *Light Scattering in Solids II*, Vol. 30 of *Topics in Applied Physics*, edited by M. Cardona and G. Güntherodt (Springer, Berlin, 1982).

¹⁹See, e.g., D. R. Frankl, *Electronic Properties of Semiconductor Surfaces* (Pergamon, New York, 1967).

²⁰See, e.g., S. M. Sze, *Physics of Semiconductor Devices* (Wiley-Interscience, New York, 1969 and 1981).

²¹D. E. Aspnes and A. A. Studna, *Phys. Rev. B* **27**, 985 (1983).

²²H. J. Stolz and G. Abstreiter, *Solid State Commun.* **36**, 857 (1980).

²³W. Franz, *Z. Naturforsch.* **13A**, 484 (1958).

²⁴L. V. Keldysh, *Zh. Eksp. Teor. Fiz.* **34**, 1138 (1958) [*Sov. Phys.—JETP* **34**, 788 (1958)].

²⁵W. Richter, in *Solid-State Physics*, Vol. 78 of *Springer Tracts in Modern Physics*, edited by G. Höhler (Springer, Berlin 1976).

²⁶W. Bludau and E. Wagner, *Phys. Rev. B* **13**, 5410 (1976).

²⁷See, e.g., E. H. Rhoderick, *Metal Semiconductor Contacts* (Clarendon, Oxford, 1978).

²⁸L. J. Brillson, R. Z. Bachrach, R. S. Bauer, and J. McMennamin, *Phys. Rev. Lett.* **42**, 397 (1979).

²⁹A. Huijser and J. van Laar, *Surf. Sci.* **52**, 202 (1975).

³⁰W. Mönch, in *Festkörperprobleme*, Vol. XXIV of *Advances in Solid State Physics*, edited by P. Grosse (Vieweg, Braunschweig, 1984), p. 229.

³¹A. Many, Y. Goldstein, and N. B. Grover, *Semiconductor Surfaces* (North-Holland, Amsterdam, 1971).

³²E. O. Johnson, *Phys. Rev.* **111**, 153 (1958).

³³J. Y. -F. Tang and J. L. Freeouf, *J. Vac. Sci. Technol. B* **2**, 459 (1984).